J Antimicrob Chemother
https://doi.org/10.1093/jac/dkac065

Journal of Antimicrobial Chemotherapy

Broad-spectrum *in vitro* activity of macrophage infectivity potentiator inhibitors against Gram-negative bacteria and *Leishmania major*

Jua Iwasaki[1,2,3], Donald D. Lorimer[4,5]†, Mirella Vivoli-Vega[6,7], Emily A. Kibble[1,8,9], Christopher S. Peacock[1], Jan Abendroth[4,5]†, Stephen J. Mayclin[4,5]†, David M. Dranow[4,5]†, Phillip G. Pierce[4,5]†, David Fox III[4,5]†, Maria Lewis[1], Nicole M. Bzdyl[1], Sofie S. Kristensen[1], Timothy J. J. Inglis[10,11], Charlene M. Kahler[1], Charles S. Bond [12], Anja Hasenkopf[13], Florian Seufert[13], Jens Schmitz[13], Laura E. Marshall[14], Andrew E. Scott[14], Isobel H. Norville[14], Peter J. Myler[4], Ulrike Holzgrabe[13], Nicholas J. Harmer [6,7] and Mitali Sarkar-Tyson[1]*

[1]Marshall Centre for Infectious Disease Research and Training, School of Biomedical Sciences, The University of Western Australia, Perth, Western Australia, 6008, Australia; [2]Wesfarmers Centre for Vaccines and Infectious Diseases, Telethon Kids Institute, University of Western Australia, Nedlands, Western Australia, 6008, Australia; [3]Centre for Child Health Research, University of Western Australia, Perth, Western Australia, 6008, Australia; [4]Seattle Structural Genomics Center for Infectious Disease, 307 Westlake Avenue North, Seattle, WA, 98109, USA; [5]Beryllium, Inc., 7869 NE Day Road West, Bainbridge Island, WA 98110, USA; [6]Department of Biosciences, Geoffrey Pope Building, Stocker Road, Exeter, EX4 4QD, UK; [7]Living Systems Institute, Stocker Road, Exeter, EX4 4QD, UK; [8]School of Veterinary and Life Sciences, Murdoch University, Perth, WA, Australia; [9]DMTC Limited, Level 2, 24 Wakefield St, Hawthorn, VIC 3122, Australia; [10]Department of Microbiology, PathWest Laboratory Medicine, Nedlands, WA 6009, Australia; [11]Medical School, University of Western Australia, Nedlands, WA 6009, Australia; [12]School of Molecular Sciences, The University of Western Australia, Perth, Western Australia, 6009, Australia; [13]Institute of Pharmacy and Food Chemistry, University of Würzburg, Am Hubland, 97074 Würzburg, Germany; [14]Defence Science and Technology Laboratory, Porton Down, Salisbury, UK

*Corresponding author. E-mail: mitali.sarkar-tyson@uwa.edu.au
†Present address: UCB Pharma, 7869 NE Day Road West, Bainbridge Island, WA, 98110, USA.

Received 8 October 2021; accepted 23 February 2022

Background: The macrophage infectivity potentiator (Mip) protein, which belongs to the immunophilin superfamily, is a peptidyl-prolyl *cis*/*trans* isomerase (PPIase) enzyme. Mip has been shown to be important for virulence in a wide range of pathogenic microorganisms. It has previously been demonstrated that small-molecule compounds designed to target Mip from the Gram-negative bacterium *Burkholderia pseudomallei* bind at the site of enzymatic activity of the protein, inhibiting the *in vitro* activity of Mip.

Objectives: In this study, co-crystallography experiments with recombinant *B. pseudomallei* Mip (BpMip) protein and Mip inhibitors, biochemical analysis and computational modelling were used to predict the efficacy of lead compounds for broad-spectrum activity against other pathogens.

Methods: Binding activity of three lead compounds targeting BpMip was verified using surface plasmon resonance spectroscopy. The determination of crystal structures of BpMip in complex with these compounds, together with molecular modelling and *in vitro* assays, was used to determine whether the compounds have broad-spectrum antimicrobial activity against pathogens.

Results: Of the three lead small-molecule compounds, two were effective in inhibiting the PPIase activity of Mip proteins from *Neisseria meningitidis*, *Klebsiella pneumoniae* and *Leishmania major*. The compounds also reduced the intracellular burden of these pathogens using *in vitro* cell infection assays.

Conclusions: These results indicate that Mip is a novel antivirulence target that can be inhibited using small-molecule compounds that prove to be promising broad-spectrum drug candidates *in vitro*. Further optimization of compounds is required for *in vivo* evaluation and future clinical applications.

Introduction

Targeting non-essential virulence factors is a rapidly emerging approach in antimicrobial drug development.[1] In contrast to antibiotics that target essential bacterial pathways, causing bactericidal or bacteriostatic effects, this strategy aims to disarm the bacteria. This enables the host to utilize its own immune defence mechanisms to eliminate the infection, resulting in reduced selection pressure.[2] One such antivirulence target is the macrophage infectivity potentiator (Mip) protein. Mip was first characterized in *Legionella pneumophila* and shown to be required for optimal intracellular infection of macrophages.[3] Subsequently, Mip orthologues have been associated with virulence in several other Gram-negative bacteria (*Burkholderia pseudomallei*,[4] *Chlamydia trachomatis*,[5] *Neisseria gonorrhoeae*[6] and *Neisseria meningitidis*[7]). A Mip protein has also been shown to participate in cell invasion of the protozoan intracellular parasite *Trypanosoma cruzi*.[8] The role of Mip in the pathogenesis of a wide range of pathogenic organisms makes this protein a promising target for novel drug development.

Mip is an immunophilin, belonging to the FK506-binding protein (FKBP) subfamily. Some orthologues (e.g. from *B. pseudomallei*) consist solely of the FKBP domain; others (e.g. from *L. pneumophila*) have an additional dimerization domain.[9] These proteins exhibit peptidyl-prolyl isomerase (PPIase) activity.[10] This enzymatic activity can be inhibited by the potent fungal macrocyclic compounds rapamycin and FK506.[11] However, the engagement of rapamycin and FK506 with the mTOR complex and calcineurin, respectively, results in immunosuppressive effects,[12,13] rendering them unsuitable for use in antimicrobial therapy. NMR analyses of *L. pneumophila* Mip protein complexed with rapamycin revealed that binding to Mip is predominantly mediated via the pipecoline moiety of the drug to the PPIase domain of Mip.[14] This study led to the design, synthesis and testing of small-molecule pipecolic acid derivatives that displayed *L. pneumophila* Mip inhibition without exerting immunosuppressive effects.[15]

Another attractive feature of Mip as an antimicrobial target is the high sequence identity of PPIase domains across species, particularly at the FK506 binding site.[16] This formed the foundation of testing of previously designed pipecolic acid derivatives against *L. pneumophila* Mip against other bacterial species, such as *B. pseudomallei*, the causative agent of melioidosis. Indeed, a select number of pipecolic acid esters from a library of compounds were demonstrated to also be efficient at inhibiting the activity of the *B. pseudomallei* Mip (BpMip) protein.[17] Similarly, the broad-spectrum activity of Mip inhibitors designed to inhibit the BpMip protein was found to be effective against the Mip of neisserial and chlamydial species *in vitro*.[7]

Previously, the detailed design and characterization of small-molecule pipecolic acid derivative compounds that can inhibit the activity of BpMip by means of a structural biology approach has been reported.[18] These compounds displayed a low micromolar affinity to BpMip and a reduction in the *in vitro* activity of BpMip in both enzymatic and cell-based infection assays. This study expands on this work to reveal three lead small-molecule compounds targeting BpMip. Binding activity of all three compounds was verified using surface plasmon resonance (SPR) spectroscopy. The determination of crystal structures of BpMip in complex with these compounds, together with molecular modelling and *in vitro* assays, demonstrated that two of the three compounds have broad-spectrum antimicrobial activity against a range of pathogens. These include Gram-negative bacteria such as *N. meningitidis* and *Klebsiella pneumoniae*, as well as the obligate intracellular parasite *Leishmania major*, which belongs to the same Kinetoplastida class of organisms as *T. cruzi*.

Materials and methods

Recombinant protein production and purification

Recombinant BpMip (strain K96243) was produced and purified as described previously.[4] The genes encoding Mip from *K. pneumoniae* (KpMip; SSGCID ID KlpnA.00130.a.B2.GE39724) and *L. major* Friedlin (LmMip; SSGCID ID LemaA.00130.a.B1.GE34425) were cloned into a BG1861 expression vector (pET-14b derivative).[19] The gene encoding Mip from *N. meningitidis* (NmMip; NMB1567) was cloned into the pET28a(+) expression vector (Novagen) with the addition of a C-terminal 6 × His tag. The protein sequences of each construct are listed in Table S1, available as Supplementary data at *JAC* Online. Plasmid DNA was transformed into *Escherichia coli* strain BL21 (DE3) pLysS. KpMip, LmMip and NmMip were recombinantly expressed and purified by HisTrap, followed by size exclusion chromatography. The details are in the Supplementary methods.

Co-crystallization and structure determination of BpMip complexes

Co-crystallization and structure determination of *B. pseudomallei* complexes was performed as described in the Supplementary methods and by Norville *et al.*[17]

B. pseudomallei SPR assay

SPR experiments were performed as described in the Supplementary methods.

PPIase assay

The PPIase assay was performed as described in the Supplementary methods and by Vivoli *et al.*[20]

Modelling

Homology modelling was performed using YASARA v19.12.14 (YASARA Biosciences).[21] Each protein was modelled using the hm_build macro, by homology to the structures of Mips from *L. pneumophila* (PDB ID: 1FD9), *T. cruzi* (1JVW; not included for the NmMip) and *B. pseudomallei* (this study), and FkpA from *E. coli* (PDB ID: 1QVH). Sequences were aligned using YASARA and curated by hand. Template structures were superimposed using PyMOL v1.8.4.2. NmMip was modelled as a dimer. Each model was then refined using the md_refine macro. Ten independent refinements were performed for each model, and the best scoring model across all refinements was selected in each case. Docking was performed using the dock_play macro, with the active-site location defined from superposition with the *B. pseudomallei* structures with compounds from this study.

B. pseudomallei cytotoxicity assays

The cytotoxicity assays were performed as described in the Supplementary methods and by Begley *et al.*[18]

N. meningitidis intracellular survival assays

Infection of Detroit 562 epithelial cells was carried out as described in the Supplementary methods and by Reimer *et al.*[7]

K. pneumoniae internalization and survival assays

Murine macrophage RAW 264.7 cells (ATCC® TIB-71™) were seeded onto 24-well tissue culture plates using 1×10^6 cells in DMEM supplemented with 10% FBS, 4 mM GlutaMAX and penicillin-streptomycin (10 000 U/mL). *K. pneumoniae* strain ST628 was harvested in 10 mL of L-15 medium supplemented with 10% FBS and GlutaMAX to an OD_{590} of 0.6–0.7. The *K. pneumoniae* culture was incubated with each inhibitor (50 μM) or DMSO control at room temperature for 1 h. RAW 264.7 cells were infected with treated *K. pneumoniae* at an moi of approximately 500:1 for 15 min at 37°C following centrifugation of the culture onto the cells at $453 \times \mathbf{g}$ for 2 min. Post-infection, the bacteria were removed by washing cells three times with PBS and treating with 1 mL of L-15 supplemented with 1 mg/mL kanamycin for 1 h at 37°C to kill any extracellular bacteria. Infected RAW 264.7 cells were lysed using 0.01% (v/v) Triton X-100 (Sigma–Aldrich) in PBS and incubated for 15 min at room temperature. Intracellular bacteria were enumerated by viable count. All results are presented as the mean of seven independent experiments containing two technical repeats. Results are expressed as the percentage of intracellular counts following inhibitor treatment relative to the vehicle control (DMSO).

L. major intracellular survival assays

Murine macrophage RAW 264.7 cells (ATCC® TIB-71™) were seeded onto 24-well tissue culture plates using 5×10^5 cells in RPMI 1640 medium (Gibco) supplemented with 10% FBS, 4 mM GlutaMAX, 100 U/mL penicillin (Gibco) and 100 mg/mL streptomycin (Gibco) and incubated for 24 h at 36°C and 5% CO_2 for 24 h to enable adherence prior to infection. *L. major* V121 axenic amastigote parasites were generated as per Zilberstein and Nitzan Koren *et al.*[22] with modifications (See Supplementary methods and the study by Zilberstein and Nitzan Koren[22]). Axenic amastigote parasites were centrifuged and resuspended at a density of 5×10^6/mL in supplemented RPMI 1640 medium and incubated with each inhibitor (50 μM) or DMSO control at 36°C and 5% CO_2 for 1 h. The medium from the cultured RAW cells was removed and 1 mL of treated parasites was added and incubated further at 36°C and 5% CO_2 for 3 h. Post-infection, the medium was removed from the RAW cells, washed twice with PBS and then cultured again with 1 mL of supplemented RPMI with 50 μM inhibitor for 24 h. Cells were harvested from the plate by scraping and 150 μL added to chamber funnels and centrifuged at $36 \times \mathbf{g}$ for 3 min onto poly-L-lysine-coated slides using a Centurion Scientific K3 cytospin. Slides were fixed in ethanol and stained using the Differential Quick stain (Amber Scientific) and visualized at 1000× magnification to check for infection. For each well, 300 randomly chosen cells were examined for infection, with percentage infected cells and the average number of parasites inside cells recorded. All results are presented as the means of nine independent experiments containing two technical repeats. Results are expressed as the percentage of cells infected with parasite.

Inhibitor cytotoxicity assays

Inhibitor-induced cytotoxicity of J774A.1 macrophage cells, Detroit 562 epithelial cells and RAW264.7 macrophage cells was measured after a 24 h incubation using the Roche LDH Cell Cytotoxicity kit (#11644793001), following the manufacturer's instructions. All results are presented as the means of five independent experiments for J774A.1 cells and three experiments for Detroit 562 and RAW264.7 cells containing two technical repeats. A positive control (Triton X-100) and negative control (media only) were included in every assay in triplicate. Results are expressed as the percentage of lactate dehydrogenase (LDH) measured in Triton X-100 for that assay.

In vivo pharmacokinetic evaluation

In vivo pharmacokinetic evaluation was performed as described in the Supplementary methods.

Statistical analyses

All statistical analyses were carried out using Mann–Whitney *U*-test and analysed using GraphPad Prism v8.

Results and discussion

Mip inhibitor design and development

A library of small-molecule compounds aiming to inhibit BpMip using the structure of rapamycin, but lacking rapamycin's immunosuppressive properties, was designed and synthesized (reviewed by Scheuplein *et al.*[23]). Three compounds from this library, SF235, SF339 and SF354, were selected for this study as their structures supported co-crystallization with Mip. SF235 (Figure 1a) and SF354 (Figure 1b) were synthesized as previously described (see Supplementary methods and the study by Seufert *et al.*[24]). In brief, a one-pot synthesis was performed starting with an amidation of nicotinic acid and the corresponding benzoic acid, respectively, under Steglich conditions, followed by an esterification with *S*-pipecolic acid (again using Steglich conditions). After *N*-deprotection, the sulphonamide was formed with benzyl sulfonyl chloride. To obtain SF339 (Figure 1c), an amidation with 3-((tert-butoxycarbonyl)amino)propanoic acid was carried out using 3,4,5-trimethoxyaniline, EDC·HCl and HOBt. The protection group was then cleaved with trifluoroacetic acid in CH_2Cl_2. The following amidation was performed using *S*-pipecolic acid, EDC·HCl and HOBt. The Boc-protection group was cleaved using trifluoroacetic acid in CH_2Cl_2. Subsequently, the sulphonamide was obtained by reaction of the free amine, DIPEA and equimolar amounts of benzyl sulfonyl chloride.

Co-crystallization studies of BpMip with Mip inhibitors

Co-crystallization trials were set up with BpMip and compounds SF235, SF339 and SF354. All these yielded crystals that diffracted to high enough resolution for structure determination (Figure 2). The N-terminal $6 \times$HisSmt tag remained attached to the protein in all three cases, with the majority of the Smt residues observed in each structure (for complete structural data see Table S2). The structure of SF235 contains four molecules per asymmetric unit, whereas the structures of SF339 and SF354 contain two molecules per asymmetric unit. In all cases the crystal lattice produces face-to-face pairs of molecules with intermolecular ligand–ligand interactions stabilizing the lattice. The pipecolic acid scaffold binding conformation previously observed[18] was retained by all three compounds with polar contacts made between the amide nitrogen of Ile63 and the carbonyl ester of all three compounds, and between the hydroxyl group of Tyr89 and one of the sulfonyl oxygens. In all three structures, we also observed the terminal phenyl ring participating in a π-edge stacking interaction with Phe43 (Figure 2).

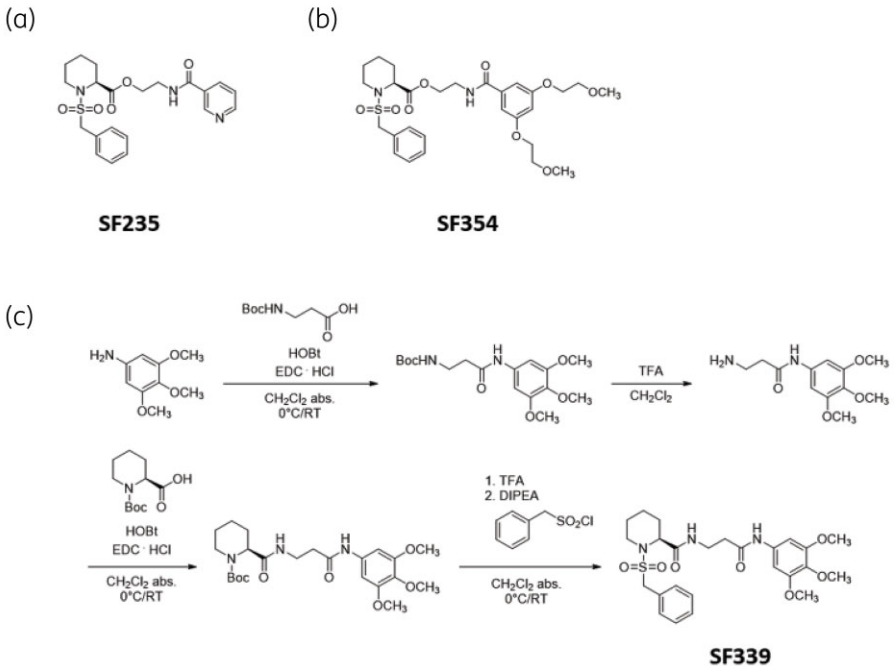

Figure 1. Structures of small-molecule compounds designed to inhibit BpMip. The synthesis of SF235 (a) and SF354 (b) have been described previously.[15,24] The synthesis of SF339 is shown (c).

SF339 adopts two poses in the structure. This results in additional interactions not observed with SF235 or SF354. In both poses, while one oxygen from the sulfonyl group is contacting Tyr89 as described above, the other sulfonyl oxygen makes a hydrogen bond to the hydroxyl of Tyr33 (Figure 2c and d). The amide adjacent to the tri-methoxy phenyl group of SF339 exists in two conformations. In one conformation (Figure 2c), the carbonyl oxygen points towards Tyr89, forming an additional hydrogen bond, which is not observed in the other conformation. Additionally, we observed an interaction between the amide nitrogen of Gly97 and one of the tri-methoxy oxygens in both poses. The extra interactions of SF339 may help to explain the lower K_i and IC_{50} values compared with SF354 (Table 1). However, despite these additional interactions, the PPIase inhibitory activity is not necessarily reproduced in a cell-based infection model.

BpMip binding to Mip inhibitors

Binding activity of the compounds SF235, SF339 and SF354 was investigated using BpMip and SPR spectroscopy. Data were processed using double referencing and analysed using steady-state affinity methods, resulting in binding affinities of 10.6 ± 0.2, 10.9 ± 0.2 and 8.9 ± 0.2 μM, respectively, for the three compounds. Double-referenced experimental data and steady-state affinity analyses are provided in Figure S6. Full steady-state analysis results are provided in Table S3.

Inhibition of BpMip PPIase activity by Mip inhibitors

The *in vitro* efficacy of SF235, SF339 and SF354 was tested using a high-throughput PPIase assay.[20] The compounds had K_i values of 290 ± 60, 450 ± 90 and 980 ± 290 nM, respectively (Table 1). The three compounds showed IC_{50} values between 260 and 580 nM, within the experimental error of K_i. This is consistent with competitive inhibition as expected from the structures.[25] These are in the same order as the most potent inhibitors that we previously identified ($K_i = 160$–1200 nM for compounds effective in cell-based assays).[18,20] This suggests that these inhibitors retain the potency of previous compounds.

Mip inhibitors SF235 and SF354 reduce B. pseudomallei virulence in vitro

Inhibition of *B. pseudomallei*-induced cytotoxicity was investigated using 50 μM SF235, SF339 and SF354 in a J774.1 macrophage cytotoxicity assay. Following infection with *B. pseudomallei*, treatment with SF235 and SF354 significantly reduced cytotoxicity by 25% compared with the DMSO-only control, as measured by LDH release from cells (Figure 3; $P < 0.01$). This reduction was similar to levels observed using a BpMip deletion mutant and previous generations of Mip inhibitors.[17] Interestingly, SF339 was less active, with no statistically significant difference detected in *B. pseudomallei*-induced cytotoxicity and was excluded from further study. This was despite this compound showing lower K_i and IC_{50} values than SF354 (Table 1). This highlights that PPIase inhibitory activity is not necessarily recapitulated in a cell-based infection model. Potentially, SF339 is less stable in cell infection models, resulting in faster degradation, which will be determined in future work. Nevertheless, the activity of Mip inhibitors SF235 and SF354 against *B. pseudomallei* highlights the potential of these two compounds as novel antibacterials for the treatment of melioidosis. Furthermore, both

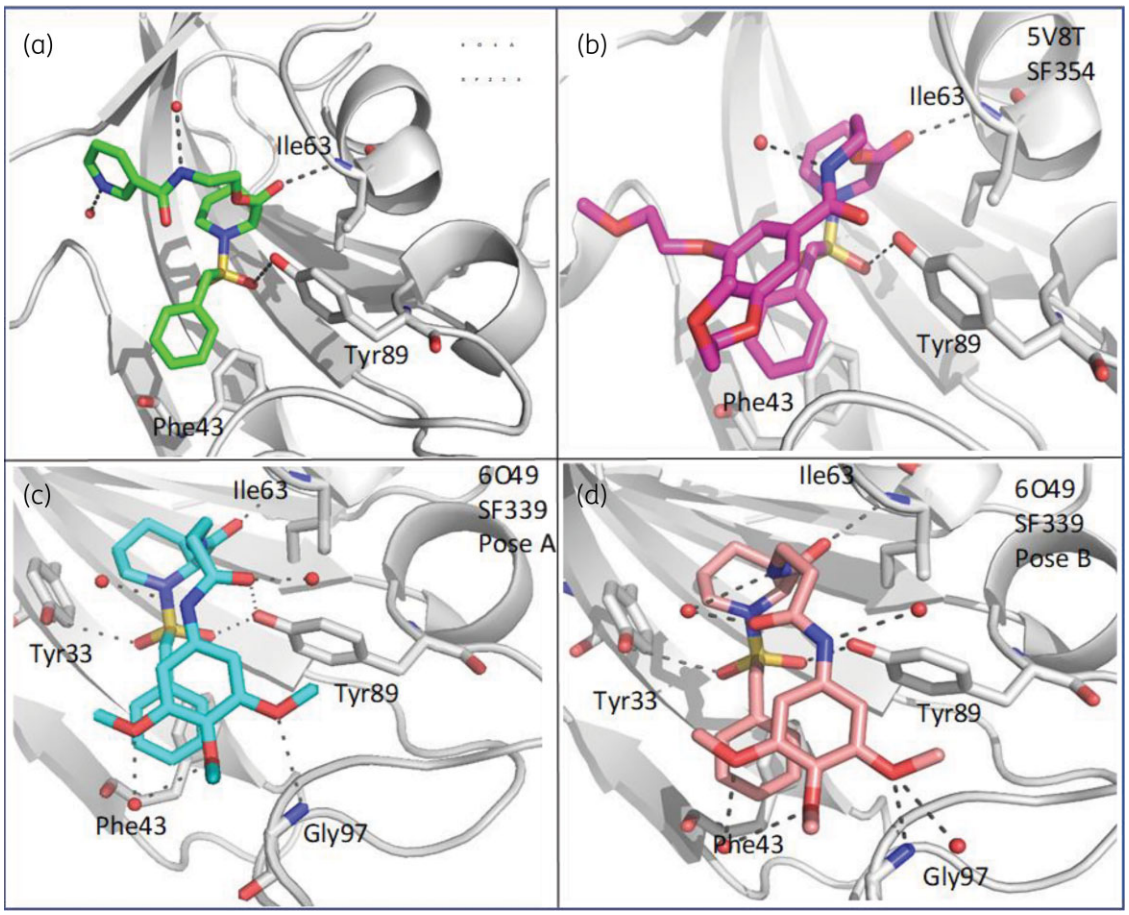

Figure 2. The active site of BpMip showing the interactions between the protein and the small molecules. SF235 (a) in green, SF354 (b) in magenta, SF339, Pose A (c) in cyan, and SF339, Pose B (d) in salmon. The protein is coloured light grey in all panels. Non-carbon atoms are coloured as follows: red, oxygen; blue, nitrogen; yellow, sulphur.

compounds induce low cytotoxicity when incubated with J774A.1 cells (Figure S1).

Computational modelling of inhibitor binding to NmMip, KpMip and LmMip proteins

To understand the potential of SF235 and SF354 as broad-spectrum Mip inhibitors, they were docked into Mip structures from several other pathogens. Mip's role in *N. meningitidis* virulence has been previously identified.[7,26] The pathogens *L. major* and *K. pneumoniae* have Mips with 47%–50% amino acid sequence identity to *B. pseudomallei* and *N. meningitidis* Mips in the PPIase domain (Figure S2). The role of Mip in these pathogens' virulence has not been investigated. The Mip proteins from *N. meningitidis*, *L. major* and *K. pneumoniae* were selected for modelling, followed by docking of SF235 and SF354 into the modelled enzymes. Homology models of *N. meningitidis*, *L. major* and *K. pneumoniae* Mips demonstrated that all three form a very similar active site to BpMip (Figure 4). SF235 and SF354 were docked into these active sites (Figure S3 and Table 2). The relative energy of docking poses similar to the structure of the compound bound to BpMip was compared with docking poses that did not reflect this structure. For LmMip, SF235 and SF354 docking poses reflecting the experimental structures had clearly higher energies than dissimilar poses. The same was true for SF235 binding to KpMip. For SF354 binding to KpMip and both ligands binding to NmMip, the highest energy docking pose reflects the ligand binding to BpMip, but there are dissimilar poses with energies that are not significantly different. This modelling suggests that SF235 and SF354 could be effective as inhibitors of Mips from all three of these pathogens.

Table 1. IC_{50} and K_i values of Mip inhibitors SF235, SF339 and SF354 against recombinant BpMip protein

	IC_{50} (μM)		K_i (μM)	
Compound	Mean	SE	Mean	SE
SF235	0.42	0.18	0.29	0.06
SF339	0.26	0.10	0.45	0.09
SF354	0.58	0.08	0.98	0.29

SE, standard error.

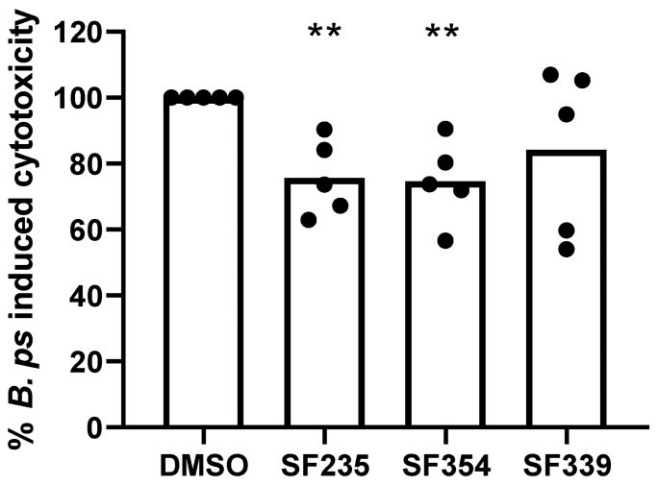

Figure 3. Mip inhibitors SF235 and SF354 reduce *B. pseudomallei*-induced cytotoxicity *in vitro*. J774A.1 cells were infected with *B. pseudomallei* K96243 treated with compounds SF235, SF354 and SF339. Cytotoxicity was measured based on LDH release, and the results are presented as the percent cytotoxicity adjusted to infected cells treated with DMSO (control). **, statistically significant, $P<0.01$, $n=5$, Mann–Whitney *U*-test. Mean and each biological replicate are shown.

However, the modelling gives higher confidence for SF235 acting on LmMip and KpMip, and SF354 acting on LmMip.

Broad-spectrum inhibition of Mip PPIase activity by SF235 and SF354

Recombinant Mip proteins from *N. meningitidis*, *K. pneumoniae* and *L. major* (all including the dimerization domain) all demonstrate PPIase activity (Figure S4). SF235 (Table 3) and SF354 (Table 4) reduce the activity of Mips from all three pathogens. Consistent with the docking results, SF235 and SF354 were effective inhibitors of LmMip ($K_i=0.9\pm0.2$ and 0.7 ± 0.1 μM for SF235 and SF354, respectively). For NmMip, both compounds were effective, but higher concentrations of SF354 were required to achieve inhibition ($K_i=1.0\pm0.2$ and 2.5 ± 0.4 μM for SF235 and SF354, respectively). Both compounds could inhibit KpMip, but substantially higher concentrations were required ($K_i=16\pm3$ and 23 ± 4 μM for SF235 and SF354, respectively). The inhibition of each of the three proteins by SF235 and SF354 is demonstrated in Figure S5. These results confirm that SF235 particularly, and SF354 to a lesser extent, have potential as broad-spectrum inhibitors. The results are largely consistent with the docking approach. Two of the three interactions with the strongest support from docking proved to give the strongest inhibition (SF235 and SF354 binding to LmMip), whilst two of the three interactions with equivocal docking support showed weaker inhibition (SF354 binding to KpMip and NmMip). This suggests that the approach of modelling and local docking is sufficiently robust to predict Mip orthologues that are likely to be inhibited by this class of compounds.

Mip inhibitors SF235 and SF354 decrease intracellular burden of N. meningitidis, K. pneumoniae and L. major in vitro

Previously, the inhibition of adherence, invasion and/or survival of *N. meningitidis* in epithelial cells in the presence of Mip inhibitors was observed.[7] However, these compounds were not suitable for therapeutic use due to low solubility. We therefore evaluated the efficacy of improved, more-soluble Mip inhibitors SF235 and SF354 against *N. meningitidis* using the same bacterial survival assay. This involved infecting epithelial cells with *N. meningitidis*

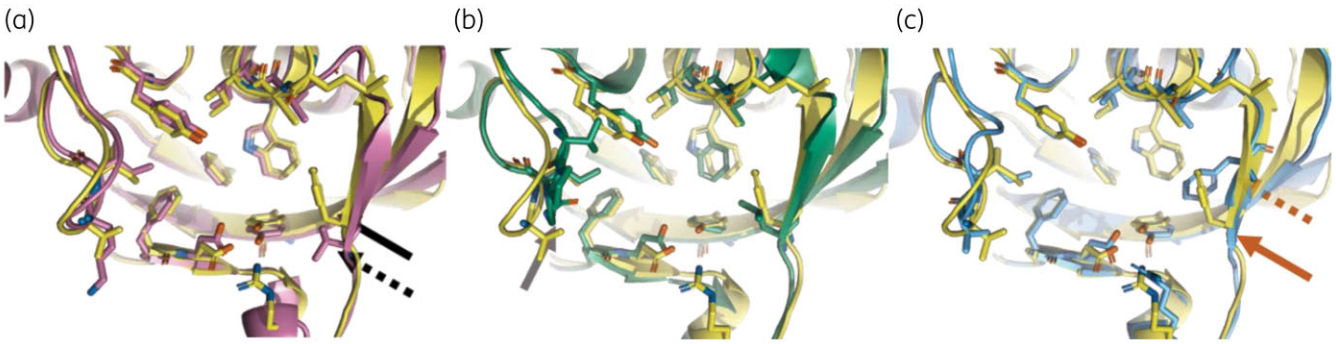

Figure 4. Mips from diverse species have similar active-site pockets to BpMip. The Mips from *N. meningitidis*, *K. pneumoniae* and *L. major* were homology modelled using YASARA. The active-site pockets were compared, focusing on amino acids within 4 Å of the position of SF235 in the BpMip structure. (a) Comparison of NmMip (magenta; oxygen atoms, red; nitrogen atoms, blue) and BpMip (yellow). NmMip has a very similar active site to BpMip, with all key amino acids binding to the compound core maintained. F53 (black arrow), on the lining of the pocket, interacts with the pyridine ring that distinguishes SF235 from other compounds in the series; this is mutated to valine (black dashed arrow), which may affect compound binding. (b) Comparison of KpMip and BpMip. The active site is again similar to BpMip. Here, the loop on the left-hand side of the pocket is drawn towards the centre of the pocket by a proline residue not found in BpMip (grey arrow); this loop interacts with the phenyl ring in the compound core, which may affect binding of this series. (c) Comparison of LmMip and BpMip. LmMip is very similar to BpMip; although F53 (orange arrow) is not conserved, a phenylalanine in a neighbouring position occupies the same space (orange dashed arrow). Proteins are shown in cartoon format with amino acids within 4 Å of SF235 shown as sticks. Image generated using the PyMOL Molecular Graphics system v.2.4.1.

Table 2. Docking of SF235 and SF354 into Mips

Species	Ligand	Pose	Binding energy (kcal/mol)	Similar to experimental?	Similar side chain?
N. meningitidis	SF235	1	6.6 ± 0.2	Yes	No
		2	6.4 ± 0.5	No	
		3	6.2 ± 0.3	Yes	Yes
		4	6.05 ± 0.08	No	
		5	6.0	No	
		6	5.9	No	
	SF354	1	6.8 ± 0.3	Yes	No
		2	6.8 ± 0.1	Yes	No
		3	6.8 ± 0.2	Yes	Yes
		4	6.8 ± 0.3	No	
		5	6.5	No	
		6	6.45 ± 0.06	No	
L. major	SF235	1	7.7 ± 0.9	Yes	Yes
		2	7.5 ± 0.9	Yes	No
		3	6.8 ± 0.2	No	
		4	6.8	No	
		5	6.7	No	
		6	6.5 ± 0.2	No	
		7	6.2	No	
	SF354	1	6.4 ± 0.3	Yes	No
		2	6.3 ± 0.5	Yes	Yes
		3	6.1 ± 0.3	Yes	No
		4	5.8	Yes	No
		5	5.6	No	
		6	5.3	No	
K. pneumoniae	SF235	1	6.6	Yes	No
		2	6.4 ± 0.2	Yes	No
		3	6.2 ± 0.3	No	
		4	6.1 ± 0.2	No	
		5	6.0 ± 0.2	No	
		6	5.9 ± 0.2	No	
	SF354	1	6.3 ± 0.1	Yes	No
		2	6.3	No	
		3	6.3 ± 0.2	No	
		4	6.1 ± 0.2	No	
		5	6.1	No	

Homology models were built of the Mips from *N. meningitidis*, *L. major* and *K. pneumoniae*, and these and the structure of Mip from *B. pseudomallei* were refined by molecular dynamics. SF235 and SF354 were docked into the active site (25 poses per compound) and the preferred poses compared with the structures of *B. pseudomallei* bound to each compound. For each preferred pose, the calculated binding energy given is the mean of similar poses sampled, with standard deviation where multiple poses were available. Docking poses were considered to reflect the *B. pseudomallei* structures if the pipecolic acid and sulphate groups occupied similar spaces; and to have a similar 'side group' if the amide-linked side group occupies a similar space to that in the *B. pseudomallei* structures. Examples of each case, and of docking poses that did not reflect the experimental structures, are provided in Figure S3. All modelling was performed using YASARA.

pre-treated with a solvent control (DMSO), SF235 or SF354 at 50 μM and determining viable bacteria and survival levels 6 h post-infection. Consistent with Reimer *et al.*,[7] the results from our present study showed that both SF235 and SF354 significantly reduced the ability of *N. meningitidis* to invade epithelial cells to approximately 30% (Figure 5a; $P < 0.01$). These findings further highlight the important role of Mip in the survival of *N. meningitidis* in epithelial cells and efficacy of SF235 and SF354 against *N. meningitidis*.

K. pneumoniae is a Gram-negative bacterium, the MDR strains of which are in urgent need of novel antibacterial therapies for treatment of infection.[27] In particular, there has been a call for new antibiotic scaffolds, such as new small molecules with meaningful cellular activity.[28] Both SF235 and SF354 significantly reduced the intracellular growth of *K. pneumoniae* (Figure 5b). Following infection of RAW 264.7 macrophage cells with a clinical isolate of *K. pneumoniae*, a 50% reduction in the number of bacteria that were internalized and survived was observed in the

Table 3. IC_{50} and K_i values of Mip inhibitor SF235 against recombinant Mip proteins of *N. meningitidis*, *K. pneumoniae* and *L. major*

	IC_{50} (μM)		K_i (μM)	
Recombinant Mip protein of:	Mean	SE	Mean	SE
N. meningitidis	0.9	0.2	1.0	0.2
K. pneumoniae	10	5	16	3
L. major	0.7	0.3	0.9	0.2

SE, standard error.

Table 4. IC_{50} and K_i values of Mip inhibitor SF354 against recombinant Mip protein of *N. meningitidis*, *K. pneumoniae* and *L. major*

	IC_{50} (μM)		K_i (μM)	
Recombinant Mip protein of:	Mean	SE	Mean	SE
N. meningitidis	2.7	0.6	2.5	0.4
K. pneumoniae	22	4	23	4
L. major	0.7	0.2	0.7	0.1

SE, standard error.

presence of SF235 (Figure 5b; $P<0.001$). Treatment with SF354 resulted in a similar effect ($P<0.05$). These results demonstrate that Mip inhibitors have activity against *K. pneumoniae*, an important cause of healthcare-related infections.

In addition to bacterial species, Mips have also been identified in intracellular parasites, reinforcing their ubiquity and their relevance for invasion and virulence. Following identification of a *T. cruzi* Mip protein, a Mip was found to be actively secreted by the parasite and is functionally involved in host cell invasion.[8] Although Mip proteins have not been fully characterized in other intracellular parasites such as *Leishmania* spp., given the close evolutionary relationship between *Trypanosoma* and *Leishmania*,[29] we hypothesized that Mips may be present in *Leishmania* and may play a role in cell invasion and intracellular parasitism. Indeed, our studies with the pathogenic *L. major* species demonstrated that Mip inhibitors SF235 and SF354 significantly reduced the percentage of infected macrophage cells compared with DMSO controls (Figure 5c; $P<0.0001$ and $P<0.0001$, respectively). These results firstly corroborate the presence of Mip in *L. major*, and secondly suggest that Mip has a role in cell invasion. The stronger effect of SF235 and SF354 against *L. major* (compared with *N. meningitidis* or *K. pneumoniae*) may reflect either the predicted extracellular location of LmMip, or the compounds' stronger inhibitory activity against this orthologue (Tables 3 and 4). Preliminary *in vivo* pharmacokinetic studies demonstrated that both SF235 and SF354 were absorbed and then metabolized within 30 min. There were no signs of toxicity (Figure S7). Further optimization of SF235 and SF354 is required for future *in vivo* evaluation of these compounds, including confirmation that they do not cause immunosuppressive effects.

In conclusion, this investigation demonstrates that antivirulence compounds against the Mip protein have broad-spectrum activity in Gram-negative bacteria and against the eukaryotic parasite *L. major*. Binding activity of three compounds with BpMip was verified using SPR spectroscopy. Based on our compound-bound crystal structures, computational modelling and biological activity, we have a strong basis for predicting a wider range of species that might be targeted by these compounds. Due to their broad-spectrum activity and low cell cytotoxicity, these compounds offer the potential as a new class of drugs against important pathogens of public health interest.

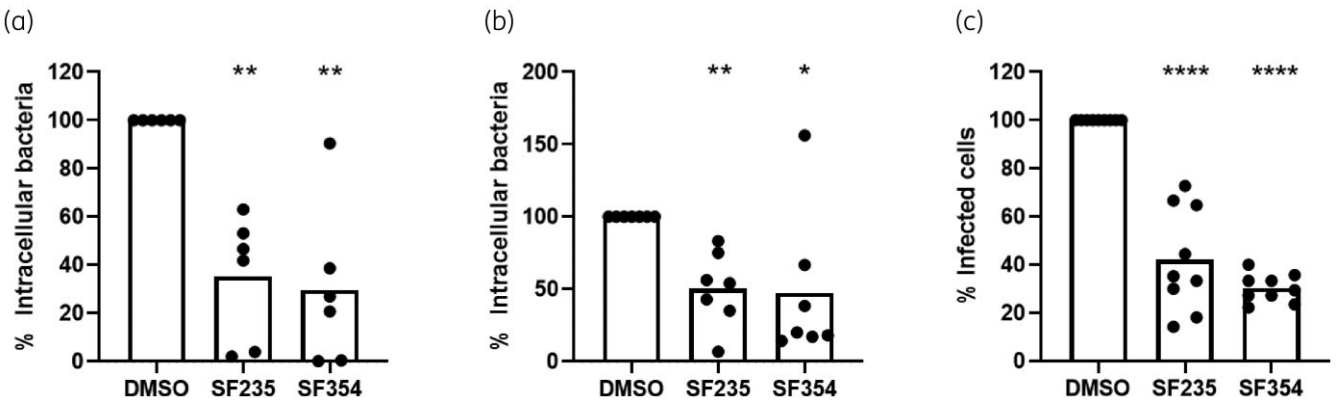

Figure 5. *In vitro* efficacy of Mip inhibitors SF235 and SF354 against (a) *N. meningitidis*, (b) *K. pneumoniae* and (c) *L. major*. *N. meningitidis* intracellular survival assays were performed on Detroit 562 epithelial cells and intracellular bacterial counts determined 6 h post-infection ($n=6$). *K. pneumoniae* internalization and survival assays were performed on murine macrophage RAW 264.7 cells ($n=7$). *L. major* intracellular survival assays were performed 3 h post-infection on RAW 264.7 cells ($n=9$). $^{*}P<0.05$; $^{**}P<0.01$; $^{****}P<0.0001$, Mann–Whitney *U*-test. Mean and individual biological replicates are shown.

Acknowledgements

Part of the research described in this paper was performed using beamline CMCF-ID at the Canadian Light Source, a national research facility of the University of Saskatchewan, which is supported by the Canada Foundation for Innovation (CFI), the Natural Sciences and Engineering Research Council (NSERC), the National Research Council (NRC), the Canadian Institutes of Health Research (CIHR), the Government of Saskatchewan and the University of Saskatchewan.

Funding

The Seattle Structural Genomics Center for Infectious Disease (SSGCID) is funded by Federal funds from the National Institute of Allergy and Infectious Diseases (NIAID), National Institutes of Health (NIH), Department of Health and Human Services, under Contracts No. HHSN272201700059C from 1 September 2017 and HHSN272201200025C from 1 September 2012 to 31 August 2017. I.H.N., N.J.H. and M.V.V. were funded by the UK Ministry of Defence. This work was supported by the North Atlantic Treaty Organization (NATO), Brussels, Belgium grant SPS 984835, and the German Research Foundation (DFG, Bonn, Germany; grant SFB 630) for the development of Mip inhibitors against *L. pneumophila* and *B. pseudomallei*, respectively, and The Federal Ministry of Education and Research for the development of Mip inhibitors against *T. cruzi* and *B. pseudomallei*, given to U.H. This paper includes research that was supported by DMTC Limited (Australia) to M.S.T., J.I. and E.A.K. The authors have prepared this paper in accordance with the intellectual property rights granted to partners from the original DMTC project.

Transparency declarations

None to declare.

Author contributions

M.S.T., U.H., P.J.M., N.J.H. and J.I. designed the study. J.I., E.A.K., M.L., N.M.B., S.S.K., D.D.L., J.A., S.J.M., D.M.D., P.G.P., D.F. III, M.V.V., N.J.H., F.S., J.S., L.E.M., A.E.S., I.H.N., C.S.P., A.H., F.S., C.S.B., T.J.J.I., C.M.K. and M.S.T. were involved in data acquisition and analysis. J.I., N.J.H., D.D.L., E.A.K., C.S.P., U.H. and M.S.T. drafted the manuscript. All authors were involved in the interpretation of the results and in drafting and/or revising the manuscript and provided final approval.

Supplementary data

Supplementary methods and references, Tables S1 to S3 and Figures S1 to S7 are available as Supplementary data at *JAC* Online.

References

1 Kolos JM, Voll AM, Bauder M *et al.* FKBP ligands—where we are and where to go? *Front Pharmacol* 2018; **9**: 1425.

2 Allen RC, Popat R, Diggle SP *et al.* Targeting virulence: can we make evolution-proof drugs? *Nat Rev Microbiol* 2014; **12**: 300–8.

3 Cianciotto NP, Eisenstein BI, Mody CH *et al.* A *Legionella pneumophila* gene encoding a species-specific surface protein potentiates initiation of intracellular infection. *Infect Immun* 1989; **57**: 1255–62.

4 Norville IH, Harmer NJ, Harding SV *et al.* A *Burkholderia pseudomallei* macrophage infectivity potentiator-like protein has rapamycin-inhibitable peptidylprolyl isomerase activity and pleiotropic effects on virulence. *Infect Immun* 2011; **79**: 4299–307.

5 Lundemose AG, Kay JE, Pearce JH. *Chlamydia trachomatis* Mip-like protein has peptidylprolyl cis/trans isomerase activity that is inhibited by FK506 and rapamycin and is implicated in initiation of chlamydial infection. *Mol Microbiol* 1993; **7**: 777–83.

6 Leuzzi R, Serino L, Scarselli M *et al.* Ng-MIP, a surface-exposed lipoprotein of *Neisseria gonorrhoeae*, has a peptidyl-prolyl cis/trans isomerase (PPIase) activity and is involved in persistence in macrophages. *Mol Microbiol* 2005; **58**: 669–81.

7 Reimer A, Seufert F, Weiwad M *et al.* Inhibitors of macrophage infectivity potentiator-like PPIases affect neisserial and chlamydial pathogenicity. *Int J Antimicrob Agents* 2016; **48**: 401–8.

8 Moro A, Ruiz-Cabello F, Fernandez-Cano A *et al.* Secretion by *Trypanosoma cruzi* of a peptidyl-prolyl *cis-trans* isomerase involved in cell infection. *EMBO J* 1995; **14**: 2483–90.

9 Riboldi-Tunnicliffe A, König B, Jessen S *et al.* Crystal structure of Mip, a prolylisomerase from *Legionella pneumophila*. *Nat Struct Mol Biol* 2001; **8**: 779–83.

10 Schiene-Fischer C, Yu C. Receptor accessory folding helper enzymes: the functional role of peptidyl prolyl cis/trans isomerases. *FEBS Lett* 2001; **495**: 1–6.

11 Hacker J, Fischer G. Immunophilins: structure-function relationship and possible role in microbial pathogenicity. *Mol Microbiol* 1993; **10**: 445–56.

12 Liu J, Farmer JD Jr, Lane WS *et al.* Calcineurin is a common target of cyclophilin-cyclosporin A and FKBP-FK506 complexes. *Cell* 1991; **66**: 807–15.

13 Ballou LM, Lin RZ. Rapamycin and mTOR kinase inhibitors. *J Chem Biol* 2008; **1**: 27–36.

14 Ceymann A, Horstmann M, Ehses P *et al.* Solution structure of the *Legionella pneumophila* Mip-rapamycin complex. *BMC Struct Biol* 2008; **8**: 17.

15 Juli C, Sippel M, Jager J *et al.* Pipecolic acid derivatives as small-molecule inhibitors of the *Legionella* MIP protein. *J Med Chem* 2011; **54**: 277–83.

16 Unal CM, Steinert M. FKBPs in bacterial infections. *Biochim Biophys Acta* 2015; **1850**: 2096–102.

17 Norville IH, O'Shea K, Sarkar-Tyson M *et al.* The structure of a *Burkholderia pseudomallei* immunophilin-inhibitor complex reveals new approaches to antimicrobial development. *Biochem J* 2011; **437**: 413–22.

18 Begley DW, Fox D 3rd, Jenner D *et al.* A structural biology approach enables the development of antimicrobials targeting bacterial immunophilins. *Antimicrob Agents Chemother* 2014; **58**: 1458–67.

19 Myler PJ, Stacy R, Stewart L *et al.* The Seattle Structural Genomics Center for Infectious Disease (SSGCID). *Infect Disord Drug Targets* 2009; **9**: 493–506.

20 Vivoli M, Renou J, Chevalier A *et al.* A miniaturized peptidyl-prolyl isomerase enzyme assay. *Anal Biochem* 2017; **536**: 59–68.

21 Krieger E, Vriend G. YASARA View - molecular graphics for all devices - from smartphones to workstations. *Bioinformatics* 2014; **30**: 2981–2.

22 Zilberstein D, Koren R N. Host-free systems for differentiation of axenic *Leishmania*. In: Clos J, ed. *Leishmania: Methods and Protocols*. Springer, 2019; 1–8.

23 Scheuplein NJ, Bzdyl NM, Kibble EA *et al.* Targeting protein folding: a novel approach for the treatment of pathogenic bacteria. *J Med Chem* 2020; **63**: 13355–88.

24 Seufert F, Kuhn M, Hein M *et al.* Development, synthesis and structure-activity-relationships of inhibitors of the macrophage infectivity

potentiator (Mip) proteins of *Legionella pneumophila* and *Burkholderia pseudomallei*. *Bioorg Med Chem* 2016; **24**: 5134–47.

25 Cer RZ, Mudunuri U, Stephens R *et al*. IC_{50}-to-K_i: a web-based tool for converting IC_{50} to K_i values for inhibitors of enzyme activity and ligand binding. *Nucleic Acids Res* 2009; **37**: W441–5.

26 Echenique-Rivera H, Muzzi A, Del Tordello E *et al*. Transcriptome analysis of *Neisseria meningitidis* in human whole blood and mutagenesis studies identify virulence factors involved in blood survival. *PLoS Pathog* 2011; **7**: e1002027.

27 Bassetti M, Righi E, Carnelutti A *et al*. Multidrug-resistant *Klebsiella pneumoniae*: challenges for treatment, prevention and infection control. *Expert Rev Anti Infect Ther* 2018; **16**: 749–61.

28 Tommasi R, Brown DG, Walkup GK *et al*. ESKAPEing the labyrinth of antibacterial discovery. *Nat Rev Drug Discov* 2015; **14**: 529–42.

29 Bartholomeu DC, de Paiva RM, Mendes TA *et al*. Unveiling the intracellular survival gene kit of trypanosomatid parasites. *PLoS Pathog* 2014; **10**: e1004399.